American Journal of Chemical Engineering
2023; 12(3): 52-63
http://www.sciencepublishinggroup.com/j/ajche
doi: 10.11648/j.ajche.20231103.12
ISSN: 2330-8605 (Print); ISSN: 2330-8613 (Online)

Modeling of Spiral Wound Membranes for CO_2 Removal from Natural Gas

Ahmed Wahba Gabr[1], Abbas Anwar Ezzat[1], A. H. EL-Shazly[2], Wael Bakr[3], Mohammed Shamakh[4], N. S. Yousef[1, *]

[1]Petrochemical Department, Faculty of Engineering, Pharos University, Alexandria, Egypt

[2]Chemicals and Petrochemicals Engineering Department, Egypt-Japan University of Science and Technology, Alexandria, Egypt

[3]Apache Co-operation Company, Gas Field Department, Cairo, Egypt

[4]Gas Lab Department, Khalda Company, Cairo, Egypt

Email address:

5320002@pua.edu.eg (Ahmed Wahba Gabr), abbas.ezzat@pua.edu.eg (Abbas Anwar Ezzat), Elshazly_a@yahoo.com (A. H. EL-Shazly), Waelbakr123@gmail.com (Wael Bakr), Mohamed.shamakh@khalda-eg.com (Mohammed Shamakh), noha.said@pua.edu.eg (N. S. Yousef)

[*]Corresponding author

To cite this article:

Ahmed Wahba Gabr, Abbas Anwar Ezzat, A. H. EL-Shazly, Wael Bakr, Mohammed Shamakh, N. S. Yousef. Modeling of Spiral Wound Membranes for CO_2 Removal from Natural Gas. *American Journal of Chemical Engineering*. Vol. 12, No. 3, 2023, pp. 52-63.
doi: 10.11648/j.ajche.20231103.12

Received: September 16, 2023; **Accepted**: October 10, 2023; **Published**: October 31, 2023

Abstract: The proposed research aims to develop an effective model and design technique for gas separation systems based on spiral-wound. Object-Oriented Programming (OOP) paradigm was applied to create a simulator of the entire membrane module used to separate CO_2 from natural gas. The simulator's architecture is represented in a Unified Modelling Language (UML) diagram, and Python was used to create it. The model was built using forward finite difference techniques in both one and two dimensions. A two-stage membrane separation machine was used to test our mathematical model. There are six banks in the primary membrane separation unit, each with seven tubes; these tubes each contain twelve membrane elements. The initial stage of a gas separation process involves introducing the gas stream, which then splits into the retentate and permeate streams. The retentate stream is discharged out as a gaseous byproduct, while the permeate stream goes via a permeate compressor to raise its pressure before entering the second stage of the membrane unit. There are ten membrane elements in each of the tubes that make up the second-stage membrane unit's membrane banks. At this point, the goal is to waste as little hydrocarbon as possible. The second-stage retentate stream is reused as feed for the first-stage reactor, while the second-stage permeate stream is directed to the flare. This two-stage membrane separation device provides an empirical test of our mathematical concept. Several tweaks have been made to our model to improve precision and computational speed. There is a new dimensionless parameter, the selectivity and permeate flow rate equations have been simplified, and faster techniques for computing key variables have been implemented. Additionally, membrane package data can be imported into the new model for a deeper dive into sensitivity analysis. Using our proposed model, we determined how changes in factors including flow velocity, pressure ratio, carbon dioxide composition, membrane active area, and membrane thickness affected product purity and CO_2 selectivity. There was an adverse relationship between product purity and feed rate, pressure ratio, CO_2 mole fraction, and membrane thickness, but a positive correlation between product purity and membrane area. The mole fraction of CO_2 also determines the selectivity for CO_2. Data collected in the field was used to verify the accuracy of the model. The validation data demonstrated that the model's predictions of MSU's performance were accurate within a margin of error of 3%.

Keywords: Membrane, Gas Separation, Spiral Wound, Mathematical Model, Forward Finite Difference, 1D Model, 2D Model

1. Introduction

Gas purification, natural gas processing, hydrogen synthesis, and carbon capture are just a few examples of the many industrial processes that rely on gas separation techniques [1]. Due to its promising qualities, such as low energy consumption, ease of operation, and environmental friendliness [2-4], membrane gas separation technology is a new technology that has garnered a lot of interest. The efficiency of a membrane separation process is largely determined by the mechanisms involved in transporting gases over the membrane [5].

When it comes to natural gas treatment and enhanced oil recovery, good mixing is essential, and spiral-wound permeators can help [6]. However, the lack of sufficient permeator models is a major bottleneck in the efficient simulation and design of membrane processes. To simplify the underlying transport models and boost the effectiveness of the strategy, approximation models based on a set of nonlinear algebraic equations have been developed [7, 8].

The process design has a significant impact on membrane economics, and single-stage systems may not be suited for more demanding applications. Mathematical programming has been used to methodically find process configuration and operating conditions, most commonly by positing a superstructure that embeds various process configurations [9, 10].

Mathematical models for characterizing membrane separation processes have evolved over time [7-24]. Early models were based on empirical relationships and experimental data, whereas more recent models are based on fundamental principles of transport processes and include detailed information about membrane structure and properties [16, 17]. Recent advancements in computational methods have enabled the development of more complex and accurate models for a wide range of membrane geometries and separations. Mathematical models have been utilized in a variety of industries to optimize process parameters, provide insights into transport phenomena, and enable the creation of more efficient and reliable separation processes. Many scientists have presented significant mathematical models to characterize membrane separation processes.

S. Weller et al. (1950) [16] proposed the fractional permeation procedure for gas separation after testing the permeability of thin organic films to various gases. The model described binary systems, but it is limited to one dimensional and unsuitable for module optimization due to the requirement of many assumptions and approximations. Pan et al. (1978) [17] devised methods for calculating multi-component gas mixture permeation and discovered that some non-ideal cascades may be more efficient. This model is also unsuitable due to many assumptions and requirements. Shindo et al. [15] presented methods for determining single-stage permeation of multicomponent gas mixtures using different flow patterns. This model assumed no pressure build up, and required many computational resources for model solving. Runhong Qi et al. (1997) [18] developed mathematical methods to simulate CO_2 removal from multicomponent mixtures of hydrocarbons but it required detailed characteristics of the membrane, which are often not known in the preliminary stage of design. A. Faizan et al. [19] developed a crossflow mathematical model and investigated how varied operating conditions and membrane selectivity affected design parameters. A. E. Amooghin et al. (2013) [20] presented a new mathematical model for evaluating ternary gas penetration across a PDMS/PA composite membrane. S. Qadir (2019) [21] proposed using membrane modules in a comprehensive computational fluid dynamics (CFD) model for natural gas separation from other gases. Due to the complexity of the model it requires the highest computational resources for solving the model. Using experimental data, R. DeJaco et al. (2020) [22] developed and validated models for gas separations with spiral-wound membranes.

A. S. Dias et al. [23] developed and tested a mathematical model to describe gas separations in spiral-wound membranes. He assumed no pressure build up in a single leaf, and used Euler function to avoid iteration. T. B. Fontoura et al. (2021) [6] proposed an improved mathematical model for gas separation with membranes that accounts for energy balance. A. Abdul-Latif (2021) [24] developed a computational model for separating multicomponent natural gas mixtures using spiral-wound membrane modules. He assumed that permeability coefficients are independent of pressure, concentration and temperature.

By developing mathematical models and design approaches for spiral-wound permeators used in gas separation systems, the proposed research will examine the fundamental gas-transport mechanisms via membranes and how they affect gas separation performance. This will be performed by creating approximate permeator models and analyzing the best operating conditions, system design, and membrane performance variables. Furthermore, mathematical programming will be applied in the research to determine the optimal process setup and operating conditions, resulting in the best process flowsheet. The findings of a comprehensive sensitivity analysis will be examined in order to comprehend the impact of membrane performance parameters on system feasibility, providing insight into the optimal design and operation of gas separation systems. The proposed research covers a large gap in existing understanding of spiral-wound permeator-based gas separation systems and has the ability to provide wide suggestions for membrane multi-stage and membrane systems construction.

2. Methods

Based on previous models established by Shindo et al. [15] and Dias et al. [23], we present an improved model for simulating membrane separation processes in this study. We made many changes to improve the model's accuracy and computational performance. The use of a new dimensionless

parameter, the simplification of equations for selectivity and mole fractions, the use of faster root finding methods, the simplification of the ODE system to linear algebraic equations, the use of the Forward Finite Difference Method [25-27] for solving, and the calculation of permeate flow rate based on retentate flow rate are some examples of these modifications.

The Object-Oriented Programming (OOP) [28-31] paradigm was used to construct the simulator of the whole membrane module for CO2 removal from natural gas in the current work. This paradigm is based on the application of the computational runtime entity principle. We also used Python software to create the simulator [28, 29, 31].

3. Mathematical Model Development

3.1. One Dimensional Mathematical Model (1-D Model)

Using basic molar balance equations and the solution-diffusion assumption, the researchers developed a 1-dimensional model to explain gas penetration across a membrane. Chemical potential gradient across membrane is expressed as concentration gradient in the model based on gas equilibrium and constant stream pressures. Several reasonable assumptions about the suggested model are made in the research as the following:

1) Conditions of steady state indicate that there has been no change in the elements influencing the segregation process and that the system has remained stable over time.
2) Gases can easily pass across the membrane without causing any sort of bulk accumulation.
3) Along the membrane leaf, there are no pressure drops.
4) The permeation mechanism is described by the solution-diffusion model.
5) The ideal gas law is respected by gases.
6) The thickness and other features of the membrane are uniform.
7) Unlike pressure and concentration, temperature is the determining factor in the permeabilities of gaseous components.
8) It's a consistent feed stream.
9) Mass transfer, thermal effects, and thermodynamic equilibrium are all taken into account.

Equations 1 and 2 are obtained by applying material balance over the differential area of the spiral wound membrane module, as the following:

$$-dF = dG \tag{1}$$

$$= dA\frac{Q_i}{\ell}\sum_{k=1}^{NC}(P_h x_k - P_l y_k) \tag{2}$$

Equation 3 is obtained by applying material balance for component i:

$$-d(x_i F) = d(y_i G) \tag{3}$$

$$= dA\frac{Q_i}{\ell}(P_h x_i - P_l y_i) \tag{4}$$

A Number of factors play a role in the equation: F, the flow rate on the high-pressure feed stream; G, the flow rate on the low-pressure permeate stream that runs perpendicular to the feed stream; NC, the number of gaseous components in the system. P_h and P_l are the feed and permeate pressures, respectively; Q_i the permeability of component i; and l is the thickness of membrane.

x_i and y_i, are the mole fractions of component i on the feed and permeate sides respectively. The following are the prerequisites that must be met:

$$\sum_{k=1}^{NC} x_k = 1 \tag{5}$$

$$\sum_{k=1}^{NC} y_k = 1 \tag{6}$$

A new term F_i, is defined by:

$$F_i = x_i F \tag{7}$$

From the inlet point to any other point, integrating Eqs. (1) and (3) gives the following:

$$G = F_f - F \tag{8}$$

$$y_i = \frac{x_{f_i}F_f - x_i F}{F_f - f}, G \neq 0 \tag{9}$$

F_f represents the inlet feed flow rate, and x_{f_i} represents the mole fraction of the feed component i.

Since it is assumed that permeate flow rate G is zero when $A = 0\ and$ by applying the L'Hospital rule in a limiting form, we calculate the mole fraction y_i at $G = 0$ and as $F \to F_f$ as the following [32].

$$y_i = \frac{\frac{Q_i}{\ell}(P_h x_i - P_l y_i)}{\sum_{k=1}^{NC}\frac{Q_k}{\ell}(P_h x_k - P_l y_k)}, G = 0 \tag{10}$$

By solving the simultaneous equations, Eq. (10), for each component, we can determine their mole fractions in the permeate stream when G = 0. Eq. (10) simplifies to the ratio of any two of its components as follows:

$$\frac{y_i}{y_j} = \frac{Q_i(P_h x_i - P_l y_i)}{Q_j(P_h x_j - P_l y_j)} \tag{11}$$

Fixing for y_i yields:

$$y_j = \frac{x_j\frac{Q_j}{Q_i}}{\frac{P_h}{P_l}\left(\frac{Q_j}{Q_i}-1\right)+\frac{x_i}{y_i}} \tag{12}$$

By Placing Eq. (12) into Eq. (6), the following equation is obtained:

$$\sum_{k=1}^{NC}\frac{x_k\frac{Q_k}{Q_i}}{\frac{P_h}{P_l}\left(\frac{Q_k}{Q_i}-1\right)+\frac{x_i}{y_i}} = 1, G = 0 \tag{13}$$

For any initial values of y_{0_i} only, Eq. (13) can be solved using Bisection's iterative approach. Using Eq. (12), we can determine the values of y_i for the remaining components. Under the condition that assuming $G \neq 0$, y_i can be calculated through the membrane area dA using Eq. (9).

The original dimensional variables are transformed into their non-dimensional representations using a suitable characteristic quantity, and this is how dimensionality-free variables are defined. The variables undergo a transformation in accordance with standard dimensional analysis concepts, yielding a new set of variables that have neither physical units nor scales. The following equations define specifically the dimensionless variables:

$$s_t = A_t \frac{Q_m P_h}{F_f \ell}, z = \frac{h_x}{L} \quad (14)$$

$$f = \frac{F}{F_f}\ f_r = \frac{F_r}{F_f} \quad (15)$$

$$\theta = 1 - f \quad (16)$$

$$g = \frac{G}{F_f} = \theta \quad (17)$$

$$q_i = \frac{Q_i}{Q_m} \quad (18)$$

$$\gamma = \frac{P_l}{P_h} \quad (19)$$

$$f_i = \frac{x_i}{f}\ g_i = \frac{y_i}{g} \quad (20)$$

The dimensionless parameters defined previously in Eq. (14) to Eq. (20) are as the following: $s_t, z, f, f_i, f_r, \theta, g, g_i, q_i, \gamma$. Q_m represents the permeability of the most permeable component; F_r represents the retentate stream flow rate; θ represents the stage cut, h_x represents the transversal lengths of retentate flux, L represents the length of the membrane element.

The following equations governing the crossflow are derived from Equations (2), (5) through (8), (10), (12), and (13) in terms of these dimensionless variables:

$$\frac{df_i}{dz} = -s_t q_i (x_i - \gamma\, y_i) \quad (21)$$

$$x_{NC} = 1 - \sum_{k=1}^{NC-1} x_k \quad (22)$$

$$\sum_{k=1}^{NC} \frac{x_k \frac{q_k}{q_i}}{\gamma\left(\frac{q_k}{q_i} - 1\right) + \frac{x_i}{y_i}} = 1\ g = 0 \quad (23)$$

$$y_j = \frac{x_j \frac{q_j}{q_i}}{\gamma\left(\frac{q_j}{q_i} - 1\right) + \frac{x_i}{y_i}}, j \neq i, NC \quad (24)$$

$$y_{NC} = 1 - \sum_{k=1}^{NC-1} y_k \quad (25)$$

$$y_i = \frac{x_{fi} - x_i f}{1 - f}, G \neq 0 \quad (26)$$

The proposed 1D model of gas separation employing a spiral wound membrane was solved using the Forward Finite Difference Method (FFDM) [25-27].

By discretizing the independent variables, the system of ordinary differential equations (ODEs) is transformed into a set of linear algebraic equations. In fluid dynamics, the upwind discretization scheme is frequently employed to take flow direction into account in cases when advection is dominate. The gas concentration at each discrete location in the domain was calculated using the upwind scheme as the dependent variable. Predictions might be produced and spiral wound membrane systems optimized for gas separation applications by applying the discretization approach and the upwind methodology to achieve an approximation of the solution to the gas separation model. The computational efficiency and practical accuracy of this method are two advantages needed for practical use.

Figure 1 represents a diagram describing the discretization method.

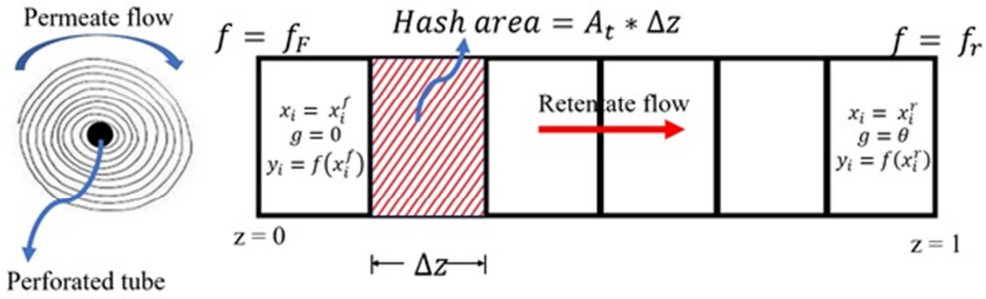

Figure 1. *Diagram For discretization method.*

The following model Equations are obtained using discretization:

$$\frac{f_i(n+1) - f_i(n)}{\Delta z} = -s_t\, q_i\big(x_i(n) - \gamma\, y_i(n)\big) \quad (27)$$

$$f(n+1) = \sum_{k=1}^{NC} f_k(n+1) \quad (28)$$

$$x_i(n+1) = \frac{f_i(n+1)}{f(n+1)} \quad (29)$$

The discretization stage is denoted by n. The following boundary condition describes a straightforward beginning value problem.

$$\begin{cases} z = 0 \rightarrow f = 1;\ x_i(z=0) = x_i^f \\ z = 1 \rightarrow f = f_r;\ x_i(z=1) = x_i^r \end{cases} \quad (30)$$

Solution algorithms:

The solution algorithm for membrane gas separation with cross flow is:

1) Input: Feed composition (x_i), permeabilities of i component (Q_i), membrane thickness (ℓ), feed flow rate (F_f), feed pressure (P_h) and permeate pressure (P_l).

2) Calculation of pressure ratio (γ) and permeabilities ratio (q_i) using Eq. (18) and (19) respectively.
3) Calculation of y_i (initial) using Eq. (23) by calling Bisection method and equation (24). Substituting $x_i = x_{f_i}$, $z = 0$ and $f = 1$.
4) Calculation of $f_i\,(n+1)$, $f(n+1)$ and $x_i(n+1)$ by using Eqs. from (27) and (29) respectively employing the same boundary condition given in equation (30). After each step, the value of $y_i(n+1)$ is changed with the new values of $x_i(n+1)$ and $f(n+1)$ in Eq. (26).
5) Proceed solving based on updated values until $z = 1$ to get x_{r_i} and y_{o_i}
6) Finally, calculation of retentate flow rate F_r, permeate flow rate G_o, and stage cut θ from Eqs. (15) to (17).

3.2. Two- Dimensional Mathematical Model (2 D Model)

Since the 1D model only included discretization along the x-axis of the membrane leaf, permeate flow rate (G) was zero. The suggested 2D model extends the discretization process along the y-axis to study permeate flow. The retentate flows is entirely in the x-direction, while the permeate flux moves in the y-direction. The elemental volume of the spiral-wound membrane module is composed of retentate and permeate sections, and the membrane layer, with retentate flux observed exclusively in the $x - direction$ and permeate flux occurring along the $y - direction$.

The suggested model makes the same assumptions as the previous model, but it also incorporates discretization along the y-axis to make it a partial differential equation (PDE) model. This results in the introduction of the four new dimensionless parameters z1, z2, sx, and sy in Equations (31) and (32), respectively.

$$s_x = A_t * h_y \frac{Q_m P_h}{F_f \ell}, s_y = A_t * h_x \frac{Q_m P_h}{F_f \ell} \quad (31)$$

$$z_1 = \frac{h_x}{L}\ z_2 = \frac{h_y}{W} \quad (32)$$

Where h_y represents the transverse length of the permeate flux.

Equations (27) to (29) acquired in the 1D model can be rewritten as follows, as can be seen in Figure 2 by shifting in the x-direction:

$$\frac{f_i(m,n+1) - f_i(m,n)}{\Delta z_1} = -s_x q_i\left(x_i(m,n) - \gamma\, y_i(m,n)\right) \quad (33)$$

$$f(m,n+1) = \sum_{k=1}^{NC} f_k(m,n+1) \quad (34)$$

$$x_i(m,n+1) = \frac{f_i(m,n+1)}{f(m,n+1)} \quad (35)$$

The values of both $g(m+1,n)$ and $g_i(m+1,n)$ can be derived from Equations (16) and (17)

$$g(m+1,n) = 1 - f(m,n) \quad (36)$$

$$g_i(m+1,n) = y_i(m,n) * g(m+1,n) \quad (37)$$

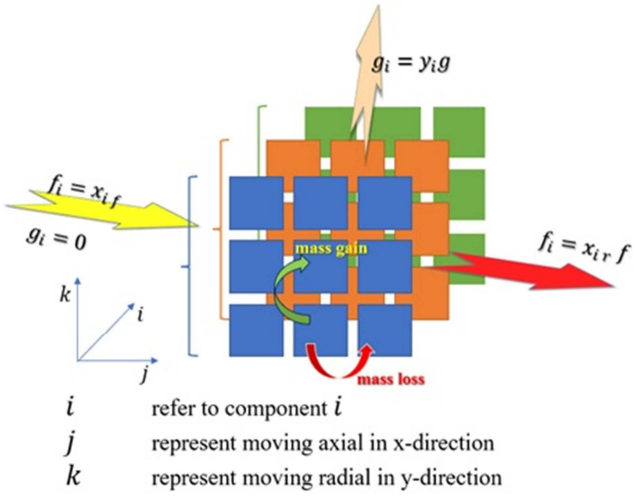

Figure 2. *Schematic representation of the proposed discretization method.*

The suggested discretization method employs the same boundary conditions used in equation (30).

Solution Algorithm:

1) The solution algorithm for membrane gas separation with cross flow is:
2) Input: Feed composition (x_i), permeabilities of i component (Q_i), membrane thickness (ℓ), feed flow rate (F_f), feed pressure (P_h) and permeate pressure (P_l).
3) Calculation of pressure ratio (γ) and permeabilities ratio (q_i) using Eq. (18) and Eq. (19) respectively.
4) Calculation of y_i (initial) using Eq. (23) by calling Bisection method and Eq. (24). Substituting $x_i = x_{f_i}$, $z = 0$ and $f = 1$.
5) Calculation of $f_i(m, n+1)$, $f(m, n+1)$ and $x_i(m, n+1)$ using Eqs. from (33) and (35) respectively employing the same boundary condition given in Eq. (30). After each step change the value of $y_i(m, n+1)$ with the new values of $x_i(m, n+1)$ and $f(m, n+1)$ in Eq. (26).
6) Proceed solving based on the updated values until $z_1 = 1$ to get x_{r_i} and y_{o_i}
7) In radial direction, $g_i(m+1, n)$ and $g(m+1, n)$ are calculated from Eqs. (36) and (37) till $z_2 = 1$.
8) Finally, at $(z_1 = z_2 = 1)$, the following are calculated: the retentate flow rate F_r, permeate flow rate G_o, and stage cut θ from Eqs. (15) to (17).

In order to create a simulator of the entire membrane module used to separate CO_2 from natural gas, Object-Oriented Programming (OOP) was put to use. The simulator's architecture is shown in the Unified Modelling Language (UML) diagram in Figure 3. The simulator was developed in Python. The simulator's class hierarchy and their interconnections are graphically represented in the UML diagram. The physical structure of the membrane was modelled using "HAS-A" relationships, and the simulator represents each level of the membrane as a class. Thus, with the specification of numerous objects, it is simple to design multiple configurations that may occur over time due to operational changes in the offshore areas.

The simulator's used classes include Each individual membrane element in the membrane module is represented by the "Element" class. Using a phenomenological model, it determines the element's mass and energy balances. Membrane qualities, operating circumstances, and the nature of the feed and permeate streams are all taken into account. Multiple membrane parts are arranged in series inside the "Tube" class, which stands for a tube. Using the mass and energy balances of the constituent materials, it determines the molar and energy balances of the tube. The permeate flow is collected in the permeate tube, while the retentate stream is used as the feed stream for the next unit in the series. The "Bank" class stands in for a group of tubes that have been laid out in parallel. It uses the mass and energy balances of the individual tubes to solve the bank's molar and energy balances. The "Stage" class stands in for a stage that features several parallel banks. All of the energy and molar balances in the stage's banks are resolved.

Each of the classes "Element," "Tube," "Bank," and "Stage" contains objects of the class that it composes, hence the four classes are related through composition. Multiple instances of the "Element" class are contained within the "Tube" class. Both the "Bank" and the "Stage" classes have many instances of the "Tube" and "Bank" classes, respectively. The "Result" class computes the relevant output variables, such as volumetric flow rates and compositions at various granularities. It takes the information it needs from the other modules and processes it. Classes like "Operational Conditions" and "Membrane Properties" rely on information from the "Parameters" and "Feed" classes, which include crucial generic parameters. It also determines how fast each molecule is being fed into the membrane module. The "Feed" type describes the incoming feed stream to the membrane module. It gives the other classes information about the input stream's composition and flow rate that they need to do their own math. The outputs of interest, such as volumetric flow rates and compositions at various levels, are computed in the classes and "Result." The simulator can accurately replicate the behavior of the whole membrane module because of the composition and inheritance interactions between these classes.

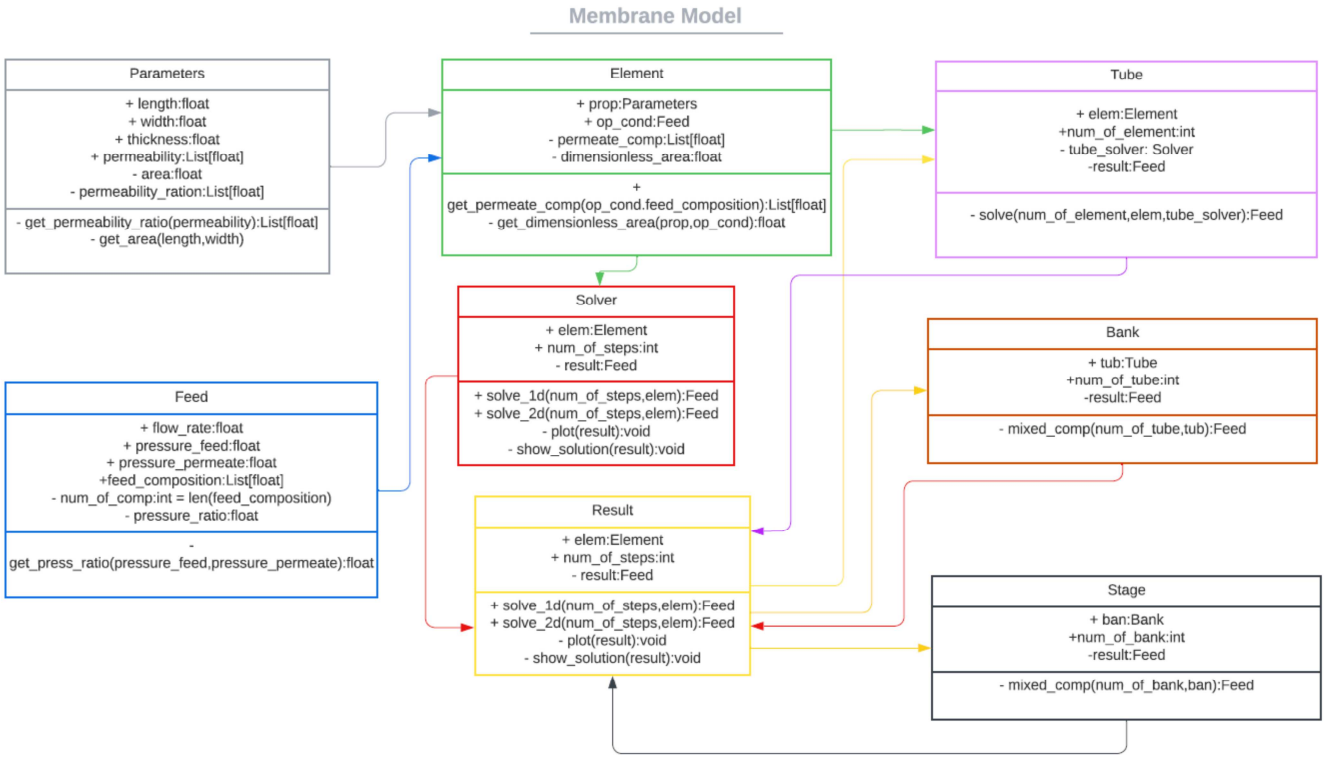

Figure 3. *UML diagram show classes in proposed model code.*

3.3. Model Validation

When working with complicated systems like gas plants, data validation is a crucial part of any research study. In order to remove CO_2 from well-produced natural gas, a treatment gas plant uses a membrane separation unit (MSU), and this study will compare estimated data to data collected from the MSU.

In this research, we used a two-stage membrane separation device to test our mathematical model. Six banks of tubes and twelve membrane elements make up the primary stage of the membrane separation unit. To begin, a gas stream that will later be split into retentate and permeate was introduced. The gaseous retentate stream is subsequently exported, while the higher-pressure permeate stream is supplied into the second stage of the membrane unit.

The second stage of the membrane unit consists of four banks, each of which has four tubes that are home to ten individual membrane elements. The containment of

hydrocarbons is its principal function. The second stage's retentate stream is returned to the first stage to be used as feed, while the permeate stream is sent to the flare. Our mathematical model is proven correct by the results of our two-stage membrane separation apparatus.

To overcome the limitation of temperature-induced permeability changes (membrane unit manufacturers only provide permeability on design temperature as proprietary information), a method was developed to obtain field data for four scenarios in which temperature was the only variable that changed. Next, a temperature-based correlation was used to forecast CO_2 permeability, and this was then used to compute the remaining permeabilities by a rearrangement of Eq. (11), thereby solving selectivity $q_{i/j}$ as follows:

$$q_{i/j} = \frac{Q_i}{Q_j} = \frac{y_i\,(P_h x_j - P_l y_j)}{y_j\,(P_h x_i - P_l y_i)} \tag{38}$$

By taking temperature's effect on permeability into consideration, we were able to achieve R^2=1, greatly enhancing the results' validity and universal applicability. To account for the inevitable variation in observed area and membrane thickness, we used average values acquired from laboratory measurements as constant values. Because of this, we were able to estimate membrane parameters with greater precision and account for their effect on system performance. By using this method, we were able to get around the lack of direct measurements of these characteristics, which increased the reliability and applicability of the findings.

Together with the field laboratory, we increased the sample rate under constant working conditions, which resolved the problem of inconsistent time intervals for data collection. Because of this, we were able to increase the frequency of our data collection to around every 30 minutes, which resulted in a more precise and trustworthy analysis. This approach helped get over the problem of varying time periods, which in turn increased the reliability and applicability of the findings.

To work around the limitation of an unreliable feed flow rate, we calculated an average over 30 minutes. This allowed us to enhance the accuracy of our estimates for the membrane parameters and account for fluctuations in flow rate.

Dimensionless lengths z in Eq. (14) and z_1 in Eq. (32) are multiplied by a flow rate adjustment factor ε to account for variations in the number of elements contained in each tube.

$$z, z_1 = \varepsilon\,\frac{h_x}{L} \tag{39}$$

Where ε is calculated as the following:

$$\varepsilon = \frac{NE_{exist}}{NE_{Max}} \tag{40}$$

In Eq. (40), NE_{exist} indicates the number of existing elements inside the tube, whereas NE_{Max} represents the maximum number of elements that the tube can hold; this corrects the total membrane length inside the tube to the real length. It allowed us to account for changes in element number and their effect on pressure and concentration gradients. We were able to produce a more accurate estimation of the membrane properties by utilizing a flow rate adjustment factor, even when the number of components differed in each tube.

A solution was created to gather samples during normal operation to overcome the limitation of back-pressure and suction impacting the feed and permeate pressures. We were able to eliminate problems caused by backpressure from the export valve and permeate compressor suction by doing so. This enabled us to produce a more precise calculation of the membrane properties and increase the results' validity and generalizability.

Table 1 shows the input data used for model validation.

Table 1. *Input data used for validation.*

Component	Q_i(mol/(m.s.Pa))	x_f
CO_2	4.35 x 10^{-11}	9.63
CH_4	1.56 x 10^{-12}	78.58
C_2H_6	7.03 x 10^{-13}	7.21
C_3H_8	2.14 x 10^{-13}	2.50
iC_4	9.44 x 10^{-14}	0.38
nC_4	1.11 x 10^{-13}	0.66
iC_5	1.13 x 10^{-13}	0.16
nC_5	1.26 x 10^{-13}	0.15
C_6^+	1.89 x 10^{-14}	0.10
N_2	1.50 x 10^{-12}	0.63
γ = 0.033		
F_f=141.9 $k(Nm^3)/hr$		
A = 37 m^2		

In Table 2, we compile the results of the 1D and 2D model validations. Mean absolute percentage error (MAPE) and coefficient of determination (R^2) were used to determine the extent of discrepancy between gas plant data and model projections.

The results of the validation research are summarized in Table 2; they demonstrate a high degree of agreement between data from the gas plant and the predictions of the proposed mathematical model. Since the MAPE was around 4%, the gap between the actual and predicted values is not too large. The model's predictions were quite close to the actual data, as measured by R^2, which was also greater than 0.9.

Table 2. *Show validation data for 1D and 2D models.*

Stages	Solver	F_r $k(Nm^3)/hr$		Err. %	x_r (CO_2)		Err. %	y_o (CO_2)		Err. %
		Exp.	Model		Exp.	Model		Exp.	Model	
1st	1D	112.46	112.61	0.13	2.97	2.84	4.38	35.06	34.96	0.29
	2D		112.24	0.19		2.87	3.37		35.21	0.43
2nd	1D	12.43	12.38	0.39	9.70	9.78	0.82	72.72	70.15	3.53
	2D		12.36	0.51		10.08	3.92		72.80	0.11

4. Results and Discussion

The primary elements that significantly affect membrane performance are the feed rate, pressure ratio, mole percentage of CO_2, membrane active area, and membrane thickness. A sensitivity analysis was performed by making small adjustments to each of these variables to learn how they affected the selectivity (q), and purity (β) for CH_4. Methane content in the retentate stream after the membrane unit is a measure of product purity, as shown in Eq. (41). The CO_2 selectivity of a membrane is measured by comparing its permeability to that of methane as the following:

$$\beta = \frac{y^o_{hyd.}}{x^f_{hyd}} = \frac{Hydrocarbon\ in\ the\ permeate}{Hydrocarbon\ in\ the\ feed} \quad (41)$$

Where $y^o_{hyd.}$ represents mole fraction of total hydrocarbon in permeate stream, x^f_{hyd} is the mole fraction of total hydrocarbon in feed stream.

4.1. Effect of Feed Flow Rate

Increasing the gas supply flow rate results in a decrease in product purity, as shown in Figure 4 (a). Product purity falls as feed rate is increased, since more hydrocarbon is introduced into the feed, and less hydrocarbon is introduced into the permeate, as a result of a shorter residence time. As seen in Figure 4 (b), as the gas feed flow rate increases, CO_2 selectivity decreases. When the input flow rate is increased, the residence period decreases, leading to less variation in CO_2 composition across the membrane and a higher CO_2 final molar composition, both of which lead to a lower CO_2 selectivity.

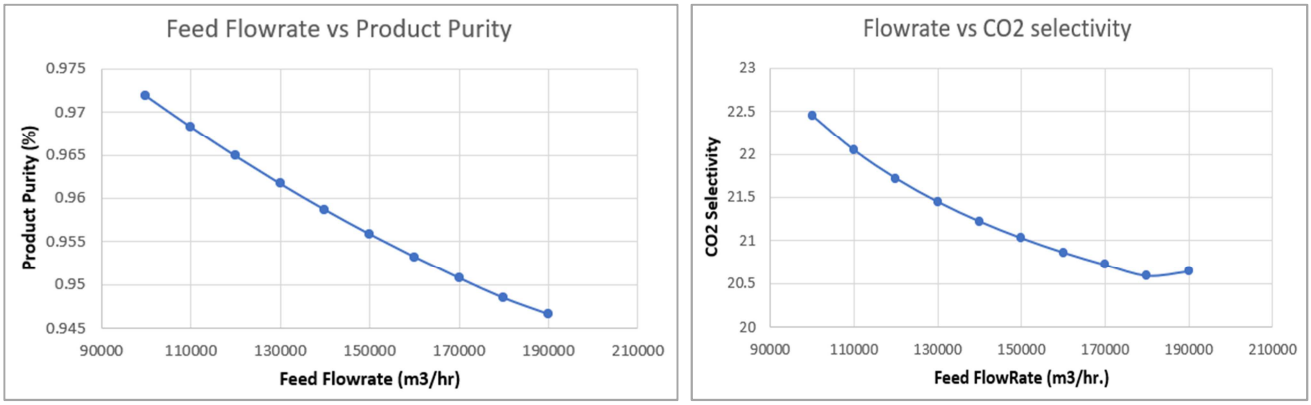

(a) (b)

Figure 4. *Effect of feed flowrate.*

4.2. Effect of Pressure Ratio

The pressure ratio is an important separation parameter because pressure differentials between streams control mass transport processes. Figure 5(a) shows that when the pressure ratio is large, the pressure gradient is small, the penetration rate is poor, and the product purity is low. Also Figure 5(b) shows that when the pressure ratio increases, the pressure gradient across the membrane decreases, leading to reduced CO_2 selectivity, and hence an increase in the ultimate molar proportion of carbon dioxide in permeate.

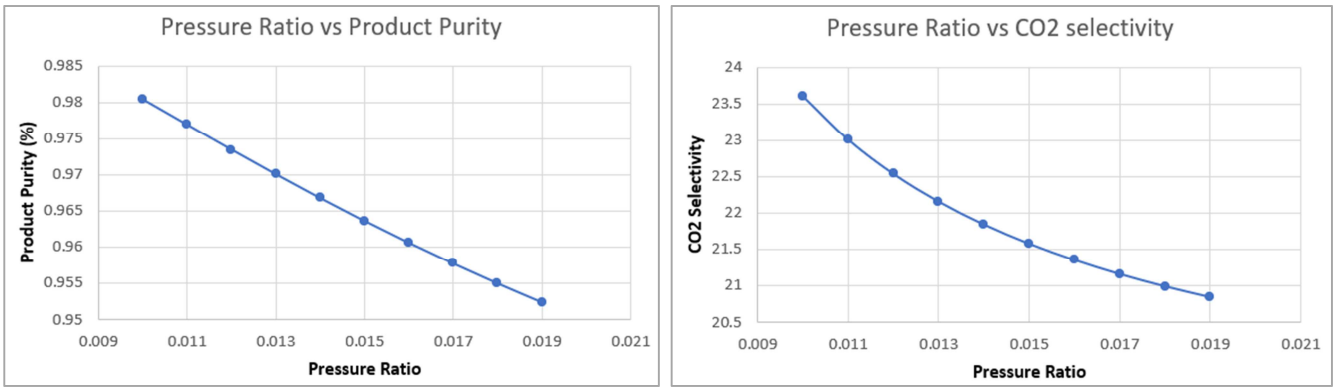

(a) (b)

Figure 5. *Effect of pressure ratio.*

4.3. Effect of Mole Fraction of CO_2 in Feed

Figure 6(a) shows that when the mole percentage of CO_2 increases, product purity declines. The purity of the final product decreases as the mole percentage of CO_2 rises because less hydrocarbon is recovered. Figure 6(b) shows that as the CO_2 mole fraction increases, the selectivity for CO_2 also increases. As the CO_2 concentration rises, the transport mechanism promotes surface diffusion because one of the molecules entering the pore wall is deposited there. This behavior restricts the pore sizes, making it hard for other molecular species to cross over. Due to its greater affinity for the membrane, carbon dioxide (CO_2) adsorbs more surface area, leaving less room for other gases. CO_2 selectivity may also be associated with the diffusion mechanism. Diffusion occurs through a semipermeable barrier, propelled by the concentration gradient. When employing a feed gas that is high in CO_2, the CO_2 is the primary driver. Because of this, it is able to cross the membrane at a much higher velocity than other gases.

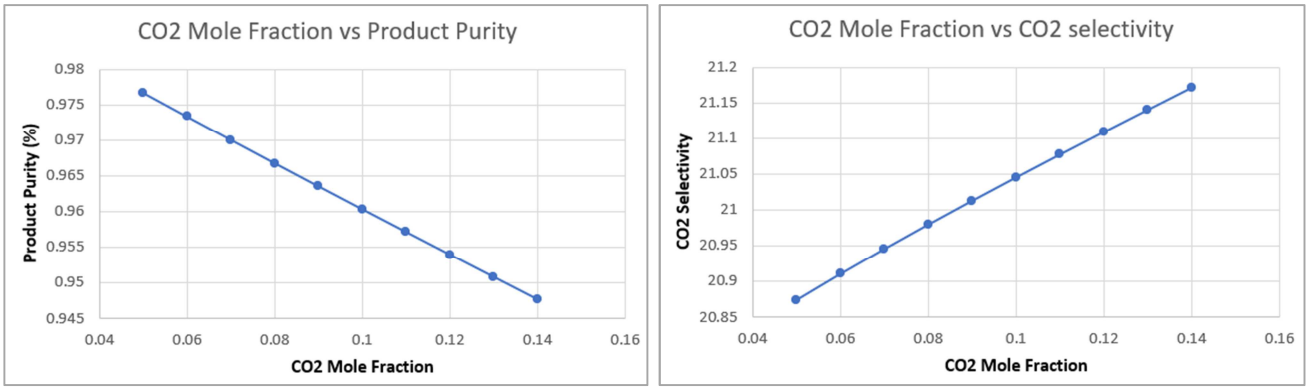

(a) (b)

Figure 6. *Effect of mole fraction of CO_2.*

4.4. Effect of Membrane Active Area

Figure 7(a) shows that when membrane active area increases, product purity improves because more selective patches form on the membrane surface, allowing the desired gas to pass through. Figure 7(b) shows that an increase in membrane active area leads to greater CO_2 selectivity because a larger active area allows more CO_2 to pass through the membrane.

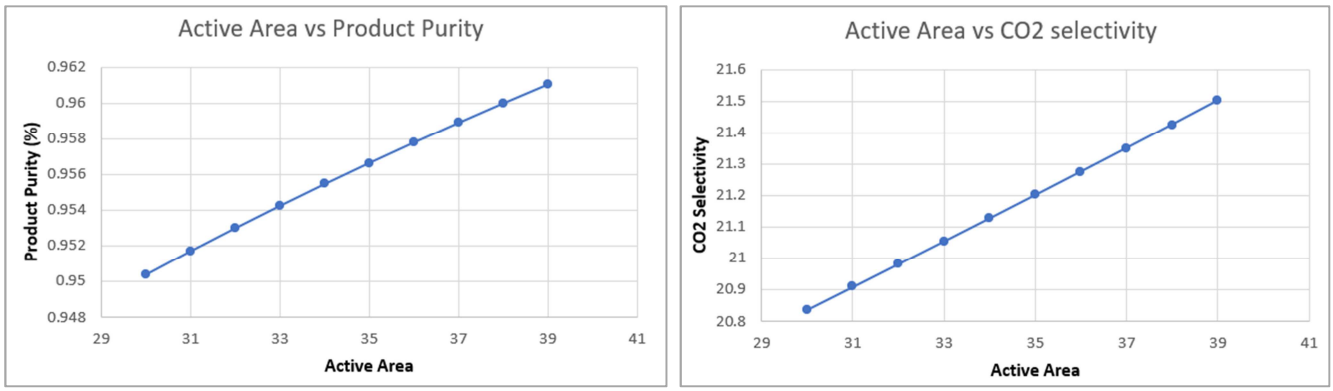

(a) (b)

Figure 7. *Effect of membrane area.*

4.5. Effect of Membrane Thickness

Increases in membrane thickness are associated with a decline in product purity, as seen in Figure 8(a). Hydrocarbon permeate is reduced and product purity is enhanced by increasing membrane thickness, as gas flux (J) and transmembrane pressure normalized flux (p) are inversely linked to membrane thickness. Figure 8(b) shows that as membrane thickness increases, CO_2 selectivity reduces because the driving force of diffusion is reduced, leading to a lower gas flux and a less amount of CO_2 passing through the membrane.

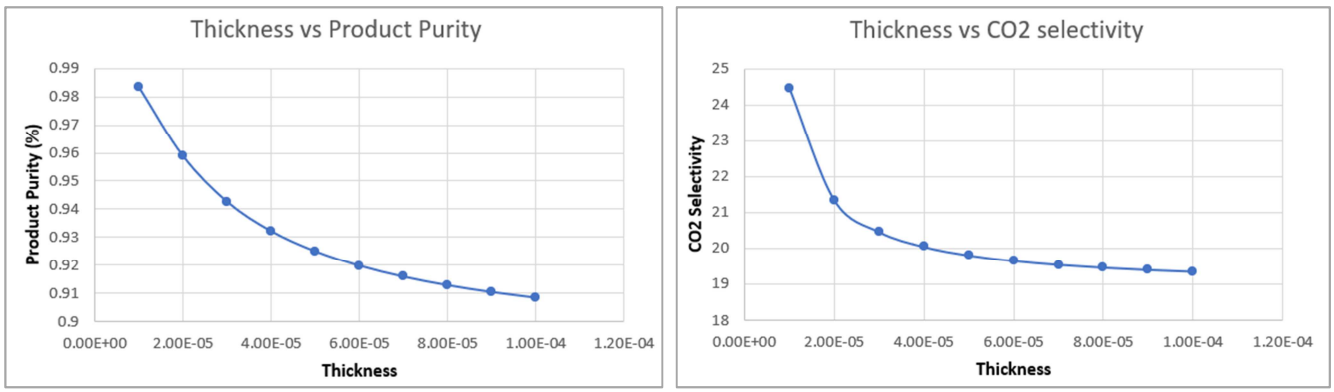

(a) (b)

Figure 8. *Effect of membrane thickness.*

5. Conclusions

To predict the performance of a Membrane Separation Unit (MSU) that use spiral-wound membranes to remove carbon dioxide (CO_2) from natural gas, a mathematical model is constructed. The model was built using forward finite difference techniques in both one and two dimensions, and it was checked against field data from a real plant. We introduce seven changes to improve the model's precision and runtime. A new dimensionless parameter is used, the selectivity and mole fraction equations are simplified, faster root finding methods are implemented, the ODE system is reduced to linear algebraic equations, the Forward Finite Difference Method is used to solve the equations, and the permeate flow rate is calculated in relation to the retentate flow rate. Our suggested model is better suited for scaling up to the membrane level and yields more accurate and efficient results.

The model accurately predicted MSU performance with a relative standard deviation of less than 3%, according to the validation data. Product purity and CO_2 selectivity were studied, along with the effects of feed rate, pressure ratio, CO_2 mole fraction, membrane active area, and membrane thickness. Feed rate, pressure ratio, Mole proportion of CO_2, and membrane thickness all had negative effects on product purity, whereas membrane area had positive effects. Additionally, CO_2 selectivity is proportional to the mole fraction of CO2.

List of Abbreviations

1D model: One-dimensional Mathematical Model
2D model: Two-dimensional mathematical Model
ODE: Ordinary differential equation
OOP: Object-Oriented Programming
FFDM: Forward Finite Difference Method
PDE: Partial differential equation
MAPE: The mean absolute percentage error
MSU: Membrane Separation Unit

Declarations

Availability of Data and Materials

Data presented in this study can be provided upon request.

Conflict of Interest

On behalf of all authors, the corresponding author states that there is no conflict of interest.

Authors' Contributions

"Ahmed Wahba Gabr is PUA Master student, and this research is obtained from his master thesis, contributed to Conceptualization, methodology, validation, investigation, resources, data curation, writing—original draft preparation, writing—review and editing. Abbas Anwar Ezzat contributed to original draft preparation, writing—review and editing, supervision. A. H. EL-Shazly is the Supervisor of Master Thesis, contributed to review and editing, supervision. Wael Bakr Said contributed to resources, data curation. Mohammed A Raheem Shamakh is contributed to 'resources, data curation. N. S. Yousef is the Supervisor of Master Thesis, contributed to Conceptualization, methodology, validation, investigation, resources, data curation, writing—original draft preparation, writing—review and editing. All authors read and approved the final manuscript"

References

[1] Bernardo, P., Drioli, E., & Golemme, G. (2009). Membrane gas separation: A review/state of the art. Industrial & Engineering Chemistry Research, 48 (10), 4638-4663. DOI: 10.1021/ie8019032.

[2] Baker, R. W. (2012). Membrane technology and applications (3rd ed.). John Wiley & Sons. ISBN: 978-0-470-74664-4.

[3] Li, Y., & Chen, H. (2018). Gas separation membranes: Polymeric and inorganic. Springer International Publishing. DOI: 10.1007/978-3-319-68255-6.

[4] Caro, J., Noack, M., Kölsch, P., & Schäfer, R. (2010). Zeolite membranes – Recent developments and progress. Microporous and Mesoporous Materials, 131 (1-3), 215-246. DOI: 10.1016/j.micromeso.2009.06.024.

[5] Liang, W., Bajpai, R., & Huang, Y. (2017). Metal–organic framework membranes for gas separation. Chemical Society Reviews, 46 (12), 3357-3385. DOI: 10.1039/C6CS00859A.

[6] Fontoura, T. B., de Sá, M. C. C., de Menezes, D. Q. F., Oechsler, B. F., Melo, A., Campos, L. F. O., Anzai, T. K., Diehl, F. C., Thompson, P. H., & Pinto, J. C. (2022). Modeling of spiral wound membranes for gas separations. Part III: A nonisothermal 2D permeation model. Chemical Engineering Research and Design, 177, 376-393. DOI: 10.1016/j.cherd.2021.10.036.

[7] Alshehri, A. A. (2015). Modeling and simulation of spiral wound membrane modules for natural gas sweetening (Doctoral dissertation). University of Waterloo. DOI: 10.20381/ruor-3459.

[8] Alshehri, A. A., & Lieuwen, D. (2021). Multicomponent spiral wound membrane model for natural gas sweetening applications. Membranes, 11 (9), 654. DOI: 10.3390/membranes11090654.

[9] Pinto, J. C., Campos, L. F. O., Melo, A., Oechsler, B. F., & Thompson, P. H. (1998). Optimization-based design of spiral-wound membrane systems for CO_2/CH_4 separation. Computers & Chemical Engineering, 22 (12), S1027-S1030. DOI: 10.1016/S0098-1354(98)00044-6.

[10] Alshehri, A. A., Lieuwen, D., & Pritzker, M. D. (2017). CO_2 removal from multi-component gas mixtures utilizing spiral-wound membrane modules: Experimental and modeling studies. International Journal of Greenhouse Gas Control, 63, 1-14. DOI: 10.1016/j.ijggc.2017.05.004.

[11] Marriott, J. I., Sørensen, E., & Bogle, I. D. L. (2001). Detailed mathematical modelling of membrane modules. Computers & Chemical Engineering, 25 (4-6), 693-700. DOI: 10.1016/S0098-1354(01)00670-6.

[12] Ang, W. L., & Mohammad, A. W. (2015). Mathematical modeling of membrane operations for water treatment. In A. Basile & A. Cassano (Eds.), Advances in membrane technologies for water treatment: Materials, processes and applications (pp. 379-407). Woodhead Publishing. DOI: 10.1016/B978-1-78242-121-4.00012-5.

[13] Alshehri, A. A., Lieuwen, D., & Pritzker, M. D. (2017). Mathematical modeling of membrane gas separation using the finite difference method. Journal of Natural Gas Science and Engineering, 38, 1-11. DOI: 10.1016/j.jngse.2016.12.002.

[14] Hébrard, G., & Lutin, F. (2013). Mathematical modelling of membrane separation. In J.-P. Canselier & M.-N. Pons (Eds.), Microemulsions: Properties and applications (pp. 233-254). CRC Press. ISBN: 9781420007129.

[15] Shindo, Y., Hwang, S. T., & Sirkar, K. K. (1985). Mathematical modelling of multicomponent membrane permeators. Journal of Membrane Science, 23 (3), 255-278. DOI: 10.1016/S0376-7388(00)80486-X.

[16] Weller, S., Hwang, S. T., & Sirkar, K. K. (1950). Permeability of thin organic films to various gases. Industrial & Engineering Chemistry, 42 (6), 1226-1231. DOI: 10.1021/ie50486a036.

[17] Pan, C. Y., Koros, W. J., & Paul, D. R. (1978). Calculation methods for multicomponent gas mixture permeation. Journal of Membrane Science, 3 (4), 351-366. DOI: 10.1016/S0376-7388(00)80257-2.

[18] Qi, R., & Henson, M. A. (1997). Mathematical modeling and simulation of CO2 removal from natural gas by membrane systems. Industrial & Engineering Chemistry Research, 36 (9), 3829-3841. DOI: 10.1021/ie960777g.

[19] Faizan, A., Al-Marzouqi, M. H., Al-Marzouqi, A. H., & Al-Hamadani, Y. A. (2010). Crossflow mathematical model for multicomponent gas separation using hollow fiber membrane modules. Journal of Membrane Science, 362 (1-2), 413-424. DOI: 10.1016/j.memsci.2010.06.057.

[20] Amooghin, A. E., Omidkhah, M. R., Kargari, A., & Moslehishad, M. (2013). Mathematical modeling of ternary gas mixture permeation through PDMS/PA composite membrane using Maxwell–Stefan approach and artificial neural network model. Chemical Engineering Research and Design, 91 (11), 2174-2187. DOI: 10.1016/j.cherd.2013.06.008.

[21] Qadir, S., Ahmad Khan, Z., & Ahmad Khan, N. A. (2019). CFD modeling of spiral wound membrane modules for natural gas separation: A review and future perspectives. Journal of Natural Gas Science and Engineering, 66, 1-14. DOI: 10.1016/j.jngse.2019.03.011.

[22] DeJaco, R. F., Thompson Jr., J. A., & Lively R. P. (2020). Modeling gas separations with spiral-wound membranes using experimental data from a commercial-scale module and a bench-scale module with identical membrane area and feed composition. Journal of Membrane Science, 598, 117689. DOI: 10.1016/j.memsci.2019.117689.

[23] Dias, A. S., Campos, L. F. O., Melo, A., Oechsler, B. F., & Pinto, J. C. (2020). Mathematical modeling of gas separations in spiral-wound membranes: Model development and validation. Chemical Engineering Research and Design, 161, 1-14. DOI: 10.1016/j.cherd.2020.05.012.

[24] Abdul-Latif, A. A. (2021). Numerical modeling of multicomponent natural gas separation using spiral-wound membrane modules (Doctoral dissertation). University of Waterloo. DOI: 10.20381/ruor-2675.

[25] Chasnov, J. R. (2022). Scientific computing. World Scientific. ISBN: 978-981-12-1339-4.

[26] Smith, G. D. (1985). Numerical solution of partial differential equations: Finite difference methods (3rd ed.). Oxford University Press. ISBN: 978-0-19-859650-9.

[27] Morton, K. W., & Mayers, D. F. (2005). Numerical solution of partial differential equations: An introduction (2nd ed.). Cambridge University Press. DOI: 10.1017/CBO9780511811268.

[28] Brett D. McLaughlin, Gary Pollice, David West (2006). Head-First Object-Oriented Analysis and Design: A Brain Friendly Guide. O'Reilly Media, ISBN: 978-0-596-00867-3.

[29] Dawson, M. (2010). Object-Oriented Programming in Python: Create Your Own Adventure Game by Michael Dawson. Course Technology PTR. ISBN: 978-1-59200-479-4.

[30] E. Balagurusamy (2008). Object-Oriented Programming with C++. McGraw-Hill Education. ISBN: 978-0-07-066907-3.

[31] Bernd Bruegge, Allen H. Dutoit (2011). Object-Oriented Software Engineering Using UML, Patterns, and Java by. Pearson Education. ISBN: 978-0-13-606125-0.

[32] Stewart, J. (2016). Calculus: Early transcendentals (8th ed.). Cengage Learning. ISBN: 978-1-305-11709-0.